Magnesium Technology 2011
Edited by: Wim H. Sillekens, Sean R. Agnew, Neale R. Neelameggham, and Suveen N. Mathaudhu
TMS (The Minerals, Metals & Materials Society), 2011

INVESTIGATION OF MICROHARDNESS AND MICROSTRUCTURE OF AZ31 ALLOY AFTER HIGH PRESSURE TORSION

Jitka Vrátná[1], Miloš Janeček[1], Josef Stráský[1], Hyoung Seop Kim[2], Eun-Yoo Yoon[2]
[1]Charles University, Department of Physics of Materials, Ke Karlovu 5, CZ-12116 Czech Republic
[2]Department of Materials Science and Engineering, POSTECH, Pohang, 790-784 Korea

Keywords: AZ31 alloy, High pressure torsion, Microhardness evolution

Abstract

Cast commercial magnesium alloy AZ31 was processed by high pressure torsion (HPT) at room temperature for 1, 3, 5 and 15 rotations (strain ranged from 1 to 7). Microstructure evolution with strain imposed by HPT was observed by light and electron microscopy. HPT was shown to be a very effective method of grain refinement. The initial coarse grain structure was refined by a factor of almost 200 already after one HPT turn ($\varepsilon \approx 4$). Mechanical properties were investigated by detailed 2-D microhardness measurements. HPT straining was found to introduce a radial inhomogeneity in the material which is manifested by a pronounced drop in the center and the maximum near the specimen periphery. With increasing strain due to HPT this inhomogeneity is continuously smeared out tending to saturate with increasing strain. Integrated 3-D meshes across the total surface of disks revealed the undulating character of microhardness variations. The strain imposed by HPT was shown to saturate with increasing number of HPT turns.

Introduction

Due to high specific strength, magnesium alloys are very attractive and promising materials for structural components in automotive and aerospace industries. However, the use of Mg alloys in more complex applications is limited because of problems associated with low ductility, poor corrosion and creep resistance. The limited ductility is a consequence of the lack of independent slip systems and the large difference in the values of the critical resolved shear stress in the potential slip systems. Moreover, the occurrence of strong deformation textures and stress anisotropy in magnesium alloys reduces significantly the variety of possible industrial applications [1].

The properties of magnesium alloys can be improved by refining the grain size to the submicrocrystalline (grain sizes in the range of 100-1000 nm) or even nanocrystalline level (grains sizes smaller than 100 nm) [2-3]. A variety of new techniques have been proposed for the production of the ultra-fine grain (UFG) structure in materials. All these techniques rely on the imposition of heavy straining and thus introduction very high density in the bulk solid material. Since these procedures introduce severe plastic deformation (SPD) into the material, it became convenient to describe all of these operations as SPD processing.

Several processes of SPD are now available but only three of them receiving the most attention at present time, in particular equal-channel angular pressing (ECAP) [4], accumulative roll-bonding (ARB) [5] and high-pressure torsion (HPT) [6].

Equal-channel angular pressing, first reported by Segal [7], became probably the most popular technique of SPD due to the combination of its effectiveness in producing UFG structure, the versatility and the scalability. Attractive results have been achieved using ECAP *e.g.* with aluminium alloys [8, 9], nevertheless the ECAP was less effective if applied to magnesium, namely dilute Mg alloys or pure Mg [10]. Recently, Horita [11] introduced a combined two-step processing route involving an initial extrusion step and subsequent processing by ECAP. This process designated by the acronym EX-ECAP, was used successfully to achieve UFG microstructures in many materials including magnesium alloys [12].

Although general principles of high pressure torsion were first proposed many years ago, it has become of general scientific interest only recently. It is only within approximately the last 5 years that numerous extensive reports documenting the processing and properties of materials fabricated by HPT have started appearing in the scientific literature showing that HPT is more effective technique of grain refinement than other SPD techniques. Extensive investigation of microstructure and mechanical properties of pure metals and solid solution alloys with FCC structure were conducted and reported in the scientific literature, e.g. in Cu [13-15], Ni [16] and Al [17-19]. Reports of successful application of HPT processing of metals with BCC structure can be found in the literature, e.g. on steels, Mo, Cr and W [20-21]. BCC metals were found to be more difficult to deform by HPT than FCC metals.

On the other hand, data about physical properties of UFG metals and alloys with hexagonal lattice are scarce. There are reports of HPT processing of titanium of commercial purity used for biomedical and dental applications [22] and zirconium for the use in surgical implants [23]. The reports describing the use of HPT with Mg alloys are almost lacking. Only recently Horita et al. reported significant grain refinement in Mg-9% Al alloy [24] and AZ61 [25].

This work is therefore motivated by this fact and its main objective is to extend this missing knowledge of the properties of UFG Mg based alloys processed by HPT. The objective of the paper is to provide a detail analysis of microstructure evolution in AZ31 alloy subjected to HPT straining and to correlate it with the observation of microstructure.

Experimental

Commercial AZ31 alloy, with a nominal composition of Mg-3%Al-1%Zn in the initial as cast condition was used in this investigation. Prior to high pressure torsion the alloy was homogenized at 390°C for 12 hours. After homogenization the disk specimens of the diameter of 20 mm and the thickness of 1 mm were cut from the billet. These specimens were processed by high pressure torsion at room temperature for 1, 3, 5 and 15 rotations by applying the hydrostatic pressure of 2.5 GPa. The experimental setup schematically illustrated at Fig. 1 comprises

two anvils. The upper anvil is fixed with a load cell mounted on its top allowing measuring the hydrostatic pressure which is applied to the specimen during straining. The lower anvil with a sample placed in the groove is first lifted to its final position pressing the specimen to the symmetrical groove in the upper anvil. Once the operating hydrostatic pressure is reached, specimen compression is stopped and maintained for 10 seconds. Then the torsional straining stage starts by rotation of the lover anvil with the constant speed of 1 rpm while maintaining the preset hydrostatic pressure.

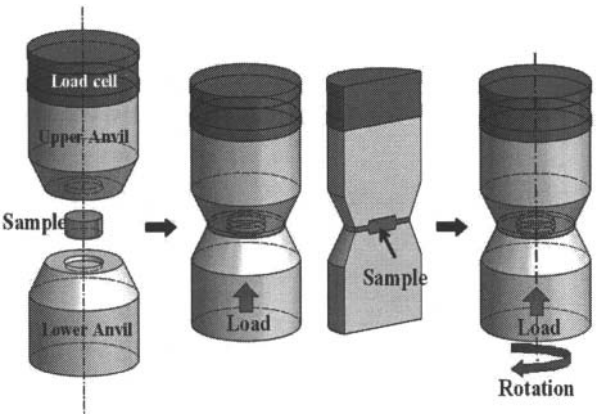

Figure 1. Schematic illustration of HPT device showing the compression and torsional stage.

Specimens for light microscopy and microhardness measurements were first mechanically grinded on watered abrasive papers, then polished with polishing suspension of grade 3 and 1 μm. Using this procedure, flat specimens with minimum surface scratches were obtained. Specimens for transmission electron microscopy were prepared by mechanical polishing followed by ion milling using PIPS ion mill at 4 kV. TEM observations were performed using Jeol 2000 FX electron microscope operated at 200 kV.

Vickers microhardness (100g load) was measured on the semi-automatic Wolpert tester allowing automatic indentation. The regular square network of indents with the step of 0.5mm was performed in one quarter of each specimen after HPT. In order to find the exact center of the specimen two additional lines of indents on the other half of the specimen were also done. In Fig. 2 the optical micrograph showing the layout of individual indents on the specimen is shown. Using this procedure the center of each specimen was found with the accuracy of +/- 0.25mm.

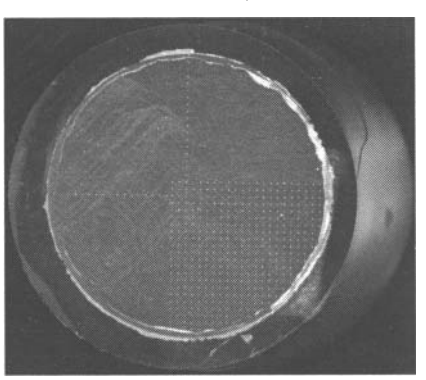

Figure 2. The square network of indents on the HPT specimen.

Results

The microstructure of AZ31 alloy in the initial condition (after homogenization treatment) is shown in Fig. 3. The microstructure consists of almost equiaxed grains with the average size of approximately 150 μm.

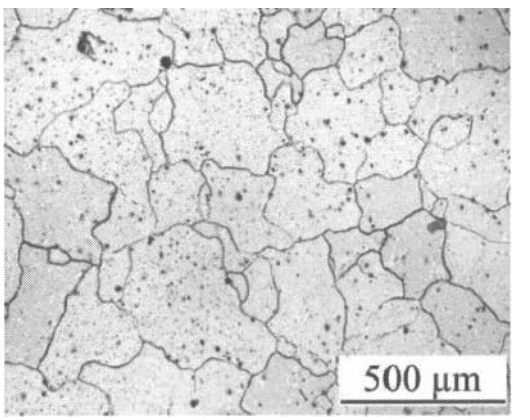

Figure 3. Microstructure of AZ31 alloy in the initial condition.

Microhardness profiles, i.e. the dependence of the microhardness on the distance r from the center of the disk were measured along two perpendicular lines passing through the center of the disc (see also Fig. 2). Fig. 4 displays the values of Vickers microhardness measured in linear traverses across the diameter of disks of AZ31 alloy after performing HPT at room temperature at different number of rotations (N=1, 3, 5 and 15). Each data point was obtained as the average of 4 Hv values obtained at the same distance from the center of the disk. The scatter of the data is in the range of approximately 10% (+/- 5 MPa). For clarity the error bars are not shown in Fig. 4. The base line of the compressed (N=0) specimen having the average value of 75 MPa is also shown in Fig. 4 to see the influence of compression and subsequent torsional straining on Hv values. Note that the average microhardness of the annealed specimen is 58 +/- 3 MPa (not shown in Fig. 4).

By detailed inspection of Fig. 4 it is seen that the initially homogeneous distribution of a compressed specimen changes. HPT staining introduces an inhomogeneity in the material which is manifested by a clear minimum in Hv values in the center of the specimen after one turn (N=1). In this specimen the microhardness increases with increasing distance from the center reaching its maxium of 110 MPa which is approximately 30 MPa higher than in the center (Hv ≈ 80 MPa). With increasing number of turns this difference gradually decreases by extension of the zone of maximum hardness from the periphery towards the center of the specimen. In the specimen after 5 turns (N=5) almost homogeneous distribution of microhardness was observed if the scatter of measured data is considered. In the specimen after 15 turns no differences in microhardness throughout the specimen were found. Note also that the maximum hardness does not change with increasing strain (number of turns). Within the experimental scatter the maximum value of approximately 112 MPa was observed in all specimens.

Microhardness results correspond well with our preliminary microstructure examinations by TEM. TEM proved significant grain refinement in specimens after HPT. One example of the microstructure is shown in Fig. 5. It displays the microstructure in the middle part of the specimen after one turn of HTP ($\varepsilon \approx 4$). It is seen that HPT resulted in strong grain refinement. New grains of the average size of approximately 800 nm are clearly seen in the micrograph. Most grains contain many dislocations. However, several recrystallized almost dislocation free grains are also seen in Fig. 5. The individual grains have high misorientation as confirmed by the contrast or by detail electron diffraction analysis.

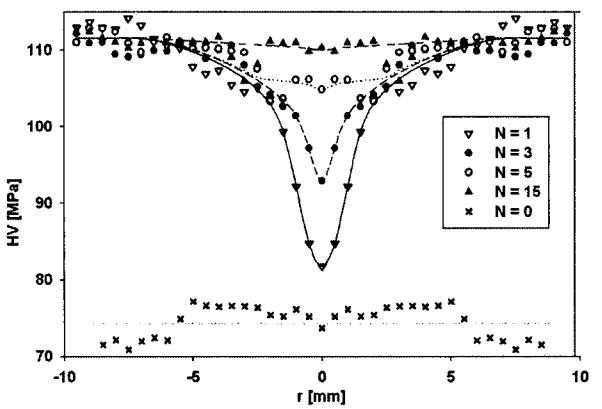

Figure 4. Microhardness distribution across the diameters of AZ31 disks subjected to a pressure of 2.5 GPa and up to 15 whole number of revolutions.

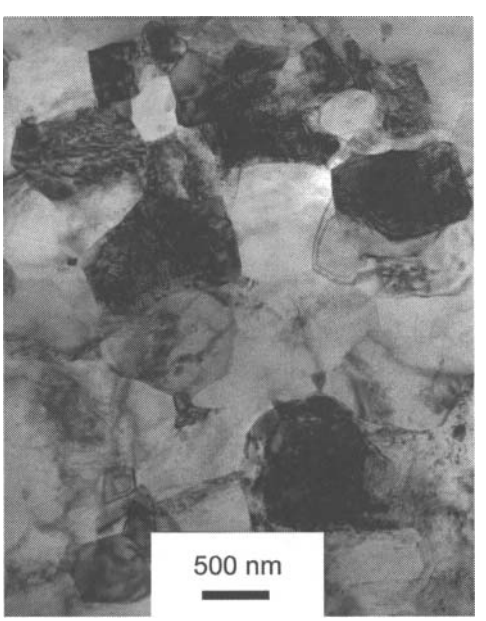

Figure 5. Typical microstructure of the specimen after 1 HPT rotation (middle section, $\varepsilon \approx 4$).

Most grain boundaries are very close to equilibrium. It is manifested by a typical thickness band structure. The detailed analysis of TEM observations in individual parts of specimens is still in progress. However, general conclusions obtained from the preliminary investigation may be summarized as follows: in the specimen after 1 turn significantly smaller grains were observed in the periphery of the disk than in the center. On the other hand, almost homogeneous distribution of grain sizes was observed in the specimen after 15 turns.

Changes of average Hv value in different parts of the disks are shown in Fig. 6 confirming the different ways towards the saturation in the center, in the middle section and at the periphery of the specimen.

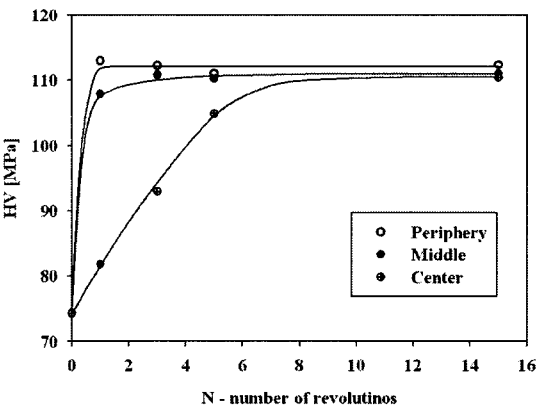

Figure 6. The evolution of average microhardness values in different parts of the disks due to HPT straining.

In order to obtain more complex image of microhardness evolution throughout individual specimens subjected to different numbers of HPT rotations three-dimensional meshes of Hv data were constructed using the following procedure. The microhardness data were measured in one quarter of each disk as described in the previous section (approximately 400-500 indents were made in each specimen). First, these data were depicted, minimal microhardness found and matched with the center of the sample. Due to the step of measurement the center of the disk was found with the accuracy of +/- 0.25 mm. Data for the whole specimen were constructed from measured data symmetrically with respect to the center (data at the same distance from the center that were measured twice were both used and the average value calculated). However, such "completed data" are not suitable for 3D-depicting. The following smoothing procedure was applied to remove each wrongly indented or evaluated datum.

Each value was recomputed using the original value and values of all close neighbors (4 edge neighbors and 4 corner neighbors). The distance of corner neighbors is $\sqrt{2}$ times higher than for edge neighbors, so the weight of corner neighbors is divided by $\sqrt{2}$ in the smoothing algorithm. Smoothing can be simply demonstrated by the following equation:

$$FV = c.OV + \frac{b}{4+2\sqrt{2}} \sum_{i=1}^{4} \left(EN_i + \frac{CN_i}{\sqrt{2}} \right) \qquad (1)$$

where FV is the final value, OV is the original value, EN is the edge neighbor, CN is the corner neighbor; fraction denominator represents partial normalization and finally c and b are smoothing parameters. However b and c are not independent (because of total normalization, i.e. $b + c = 1$). Thus only e.g. c can be

arbitrarily chosen. The choice $c = 1$ means that no smoothing occurs, whereas minimal meaningful value of c is 0.12. Otherwise the weight of each edge neighbor is higher than the weight of original values. In our case the value of $c = 0.3$ was used. It corresponds to the weight of 0.3, 0.1 and 0.07 for the original value, the edge neighbor and the corner neighbor, respectively.

Equation (1) holds only for interior points (a point that has all eight neighbors). Points that have incomplete number of neighbors are treated in the manner that nonexistent neighbors are ignored and weights of others are appropriately adjusted. Similarly, this procedure allows healing the missing data from the interior of the sample. The procedure extrapolates any missing value from values of the neighbors (if at least 5 of 8 possible neighbors exist). This procedure allows depicting 3D plots in a readable way even for partly damaged and/or missing data.

Unlike Fig. 4 which is based on taking measurements of the variation in the microhardness values following diameters across disks after HPT processing, Fig. 7 shows integrated data across the total surface of individual disks. In Fig. 7 three-dimensional meshes of microhardness for specimens subjected to different number of turns are displayed. These plots were obtained by symmetrical completion of measured data and by smoothing procedure described in the previous paragraph. The variations of microhardness with position within the disk are clearly displayed at these meshes. The pronounced drop of microhardness in the center of the specimen after one turn is clearly seen in Fig. 7a. In the specimen after 3 turns (Fig. 7b) the central drop is still visible even if its depth is much lower in comparison with the specimen after 1 turn. The tendency to saturation with increasing number of turns is demonstrated at the mesh for the specimen after 15 turns (see Fig. 7c) whose surface is almost flat with slight undulations only, confirming saturated Hv values within the whole specimen.

Discussion

Microhardness Behavior and the Development of Homogeneity in AZ31

The variations in the values of microhardness across the diameters of AZ31 disks processed by HPT are in full agreement with the well-known dichotomic behavior reported by other authors in materials with face centered cubic structure and low stacking fault energy, e.g austenitic steel [26], Cu [27] and Ni [28]: i) lower hardness values were reported in the centers of disks and higher values in peripheral regions and ii) when torsional straining is continued to a sufficiently high total strain these variations tend to saturate and almost homogeneous microhardness distribution throughout the diameter of the disk is observed. Inspecting Fig. 6 shows that the saturation is achieved after 5 HPT rotations. As reported by Somekawa et al. [29] AZ31 alloy has a stacking fault energy of 27.8 mJm^{-2}. Our measurements indicate that it is the stacking fault energy rather than the lattice structure which controls the microstructure evolution of the material which is macroscopically manifested by microhardness behavior. Contrary to these results, the centers of disks for pure aluminum exhibit higher values of Hv than the surroundings areas in early stages of torsional straining [30]. The authors explain this inverse behavior by exceptionally high rate of dynamic recovery in this material. Relatively low rate of dynamic recovery may be therefore expected in AZ31 alloy.

Detail inspection of 3D meshes in Fig. 7 reveals the undulating character of microhardness variations across HPT disks indicating the manner in which the deformation develops in AZ31 alloy. This problem was recently addressed by strain gradient plasticity modeling introduced by Estrin et al. [31]. The authors consider the material in the form of a composite material comprising cell walls and cell interiors. The dynamic recovery in the former occurs by climbing of dislocations whereas in the latter it is the cross slip of dislocations which controls the rate of dynamic recovery. The cross slip in AZ31 is very difficult due to high separation width between partial dislocations. For a low stacking fault energy material the model predicts the behavior observed in Fig. 4 with clear minimum in the center of the disk in early stages of straining tending to saturate with continuing deformation.

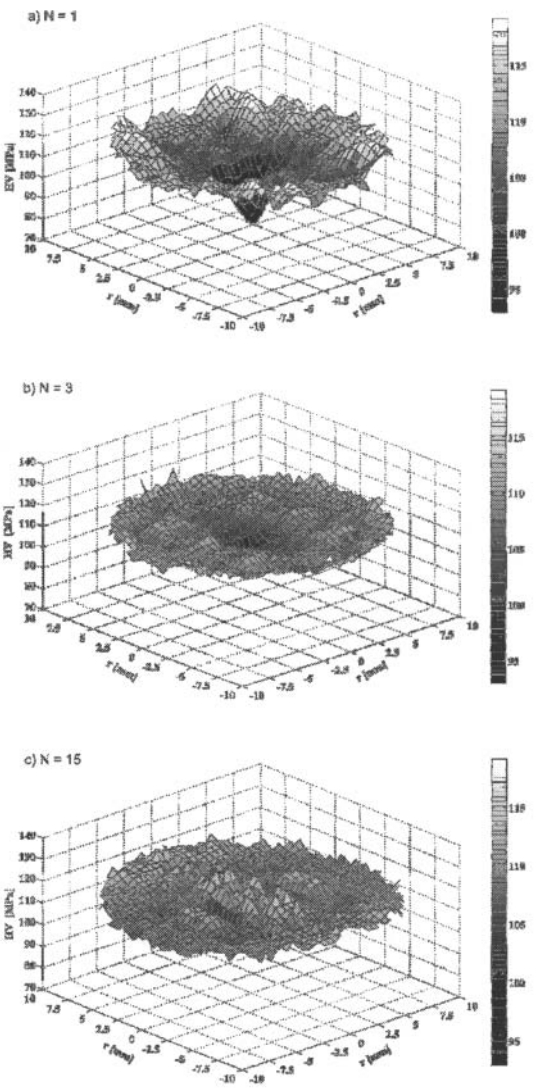

Figure 7. Three- dimensional meshes of microhardness as a function of the number of turns: a) N=1 turn, b) N=3 turns, c) N=15 turns.

Strain imposed by HPT

Due to the variability in strain across the radius of torsionally strained specimen there were many attempts how to express the strain imposed by HPT in terms of the radius of the disk and the number of HPT rotations.

Exhaustive discussion of the definition of strain imposed during HPT processing allowing calculation of different strain types (the true accumulated strain, shear strain, equivalent von Mises strain, the equivalent strain and the true strain) using different models can be found in the review by Zhilyaev [32].

The most precise quantity, taking directly into account the change of the specimen thickness during HPT processing, is the true strain ε defined as:

$$\varepsilon = \ln\left[1+\left(\frac{2\pi N.r}{h}\right)^2\right]^{\frac{1}{2}} + \ln\left(\frac{h_0}{h}\right), \qquad (2)$$

where N is number of revolutions, r is radius of the specimen, h_0 and h is the original and final thickness of the specimen, respectively. The first term of the equation (2) corresponds to the torsion of the specimen, whereas the second term refers to the compression strain due to thickness reduction.

The initial thickness h_0 of samples before HPT was 1 mm. The final thickness h of samples depends slightly on the number of HPT turns. Table I summarizes the values of final thickness of specimens after different number of HPT turns obtained as the average of thickness measurements at four specimens in the same condition. As the volume of the sample does not change significantly, the final thickness decrease was caused by outward flow of material due to a quasi-constrained setup of HPT anvils.

Table I. The dependence of the final thickness of HPT specimens on the number of turns.

N	h [mm]
0	1
1	0.8
3	0.76
5	0.75
15	0.74

The theoretical dependence of strain on the number of revolutions calculated according to eq. (2) is shown in Fig. 8. Radii under consideration are 10 mm (the periphery of the sample), 5 mm (middle section) and 0.25 mm (the center - it is the approximate value of the distance from sample center at which the closest microhardness value could have been measured). It is of particular interest that the strain saturates very soon (after 3 revolutions), especially for peripheral and middle regions. To illustrate this: another two revolutions (3 together) do not cause the strain of peripheral and middle section to rise for more than one third of the strain imposed after the first revolution. On the other hand, by second and third revolution the strain imposed in the center doubles. Similar relations hold between 3 and 15 revolutions. By straining the sample for additional 14 rotations (15 altogether) the imposed strain on the periphery and in the middle doubled only as compared to the strain after one rotation. Whereas by additional 14 rotations the imposed strain in the center tripled with respect to the strain after one rotation.

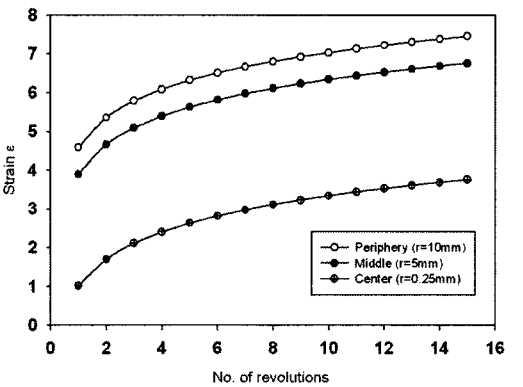

Figure 8 Dependence of the true strain on the number of HPT rotations in various parts of the specimen.

Conclusions

The influence of HPT straining on microhardness evolution and microstructure in cast magnesium alloy AZ31 was investigated. The following conclusions may be drawn from this work.

- HPT straining results in strong grain refinement.
- HPT straining introduces a radial inhomogeneity in the material with a pronounced minimum in the center and the maximum near specimen periphery.
- The inhomogeneity in Hv is continuously smeared out with increasing number of turns by continuous extension of the zone of maximum hardness towards the specimen center.
- The integrated Hv data across the whole surface of HPT specimens revealed undulating character of microhardness variations across HPT disks.
- The rate of dynamic recovery in AZ31 is very low due to its the low stacking fault energy.
- Preliminary observations of microstructure evolution correspond well with microhardness behavior.

Acknowledgements

The authors acknowledge funding through the research program MSM 0021620834 of Ministry of Education of the CR. Partial support by GACR under grant 106/09/0482 is also gratefully acknowledged. J. Vrátná acknowledges financial support by GAUK under the Grant 9594/2009 and by Grant SVV-261303.

References

1. S.R. Agnew, J.A. Horton, T.M. Lillo and D.W. Brown, "Enhanced Ductility in Strongly Textured Magnesium Produced by Equal Channel Angular (ECA) Processing", *Scripta Materialia*, 50 (2004), 377-381.

2. Y. Estrin, S.B.Yi, H.G. Brokmeier, Z. Zúberova, S.C. Yoon, H.S. Kim, R.J. Hellmig, "Microstructure, texture and mechanical properties of the magnesium alloy AZ31 processed by ECAP", *International Journal of Materials Research*, 99 (2008), 50-55.

3. R.B. Figueiredo, T.G. Langdon, "The characteristics of superplastic flow in a magnesium alloy processed by ECAP", *International Journal of Materials Research*, 100 (2009), 843-846.

4. R.Z. Valiev, T.G. Langdon, "Principles of equal-channel angular pressing as a processing tool for grain refinement", *Progress in Materials Science,* 51 (2006), 881-981.
5. Y. Saito, N. Tsuji, H. Utsunomiya, T. Sakai, R.G. Hong, "Ultra-fine grained bulk aluminum produced by accumulative roll-bonding (ARB) process", *Scripta Materialia,* 39 (1998), 1221-1227.
6. N.A. Smirnova, V.I. Levit, V.I. Pilyugin, R.I. Kuznetsov, L.S. Davydova, V.A. Sazonova, "Evolution of the structure of f.c.c. single crystal subjected to strong plastic deformation", *Fizika Metallov i Metallovedeniya,* 61 (1986), 1170–1177.
7. V.M. Segal, "Materials processing by a simple shear", *Mater. Sci. Eng.*, A 197 (1995), 157-164.
8. R.Z.Valiev, D.A Salimonenko, N.K. Tsenev, P.B. Berbon, T.G. Langdon, "Observations of high strain rate superplasticity in commercial aluminium alloys with ultrafine grain sizes", *Scripta Materialia,* 37 (1997), 1945-1950.
9. Z. Horita, M. Furukawa, M. Nemoto, A.J. Barnes, T.G. Langdon, "Superplastic forming at high strain rates after severe plastic deformation", *Acta Materialia*, 48 (2000), 3633-3640.
10. A. Yamashita, Z. Horita, T.G. Langdon, "Improving the mechanical properties of magnesium and magnesium alloy through severe plastic deformation", *Materials Science and Engineering*, A 300 (2001), 142-147.
11. Z. Horita, K. Matsubara, T.G. Langdon, "A two-step processing route for achieving a superplastic forming capability in dilute magnesium alloys", *Scripta Materialia,* 47 (2002), 255-260.
12. K. Matsubara, Y. Miyahara, Z. Horita, T.G. Langdon, "Developing superplasticity in a magnesium alloy through a combination of extrusion and ECAP", *Acta Materialia*, 51 (2003), 3073-3084.
13. Z. Horita, T.G. Langdon, "Microstructures and microhardness of an aluminum alloy and pure copper after processing by high-pressure torsion", *Materials Science and Engineering*, A 410–411 (2005), 422-425.
14. Z. Horita, D.J. Smith, M. Nemoto, R.Z. Valiev, T.G. Langdon, "Observations of grain boundary structure in submicrometer-grained Cu and Ni using high-resolution electron microscopy", *Journal of Materials Research,* 13 (1998), 446-450.
15. Y.H. Zhao, Y.T. Zhu, X.Z. Liao, Z. Horita, T.G. Langdon, "Influence of stacking fault energy on the minimum grain size achieved in severe plastic deformation", *Materials Science and Engineering, A* 463 (2007), 22-26.
16. A.P. Zhilyaev, G.V. Nurislamova, B.K. Kim, M.D. Baró, J.A. Szpunar, T.G. Langdon, "Experimental parameters influencing grain refinement and microstructural evolution during high-pressure torsion", *Acta Materialia*, 51 (2003), 753-765.
17. Z. Horita, D.J. Smith, M. Furukawa, M. Nemoto, R.Z. Valiev, T.G. Langdon, "An investigation of grain boundaries in submicrometer-grain Al_Mg solid solution alloys using high-resolution electron microscopy", *Journal of Materials Research,* 11 (1996), 1880-1890.
18. G, Sakai, Z, Horita, T,G. Langdon, "Grain refinement and superplasticity in an aluminum alloy processed by high-pressure torsion", *Materials Science and Engineering*, A 393 (2005), 344-353.
19. S. Dobatkin, E.N. Bastarache, G. Sakai, T. Fujita, Z. Horita, T.G. Langdon, "Grain refinement and superplastic flow in an aluminum alloy processed by high-pressure torsion", *Materials Science and Engineering*, A 408 (2005), 141-146.
20. Y.U. Ivanisenko, I. MacLaren, X. Sauvage, R.Z.Valiev, H.J. Fecht, "Shear-induced $\alpha \rightarrow \gamma$ transformation in nanoscale Fe–C composite", *Acta Materialia,* 54 (2006), 1659-1669.
21. S.S.M. Tavares, D. Gunderov, V. Stolyarov, J.M. Neto, "Phase transformation induced by severe plastic deformation in the AISI 304L stainless steel", *Materials Science and Engineering*, A 358 (2003), 32-36.
22. J. Petruželka, L. Dluhoš, D. Hrušak, J. Sochova, "Nanostructure titanium – new material for dental implants (in Czech)", *Česká Stomatologická Ročenka,* 106 (2006), 72-77.
23. L. Saldana, A. Mendez-Vilas, L. Jiang, M. Multigner, J.L. Gonzalez-Carrasco, M.T. Perez-Prado et al. "In vitro biocompatibility of an ultrafine grained zirconium", *Biomaterials,* 28 (2007), 4343-4354.
24. M. Kai, Z. Horita, T.G. Langdon, "Developing grain refinement and superplasticity in a magnesium alloy processed by high-pressure torsion", *Materials Science and Engineering*, A 488 (2008), 117-124.
25. Y. Harai, M. Kai, K. Kaneko, Z. Horita, T.G. Langdon, "Microstructural and Mechanical Characteristics of an AZ61 Magnesium Alloy Processed by High-Pressure Torsion", *Materials Transactions,* 49 (2008), 76-83.
26. A. Vorhauer, R. Pippan, "On the homogeneity of deformation by high pressure torsion," *Scripta Materialia*, 51 (2004), 921-925.
27. H. Jiang, Y.T. Zhu, D.P. Butt, I.V. Alexandrov, T.C. Lowe, "Microstructural evolution, microhardness and thermal stability of HPT - processed Cu", *Materials Science and Engineering*, A 290 (2000) 128-138.
28. Z. Yang, U. Welzel, "Microstructure–microhardness relation of nanostructured Ni produced by high-pressure torsion", *Materials Letters*, 59 (2005), 3406-3409.
29. H. Somekawa, K. Hirai, H. Watanabe, Y. Takigawa, K. Higashi, "Dislocation creep behavior in Mg–Al–Zn alloys", *Materials Science and Engineering*, A 407 (2005), 53-61.
30. C. Xu, Z. Horita, T.G. Langdon, "The evolution of homogeneity in processing by high-pressure torsion", *Acta Materialia*, 55 (2007), 203-212.
31. Y. Estrin, A. Molotnikov, C.H.J. Davies, R. Lapovok, "Strain gradient plasticity modelling of high-pressure torsion", *Journal of the Mechanics and Physics of Solids*, 56 (2008), 1186-1202.
32. A.P. Zhilyaev, T.G. Langdon, "Using high/pressure torsion for metal processing: Fundamentals and applications", *Progress in Materials Science,* 53 (2008), 893-979.